Judith Peñas Farré

SYNTHESIS OF GOLD NANOSTARS COATED WITH A SILVER LAYER

MASTER'S DEGREE THESIS

Supervised by Dr.Nicolás Pazos Pérez, Dr. Luca Guerrini, and Prof. Xavier Mateos Ferré

MASTER'S DEGREE IN NANOSCIENCE, MATERIALS AND PROCESSES

UNIVERSITAT ROVIRA i VIRGILI

Tarragona

2024

SYNTHESIS OF GOLD NANOSTARS COATED WITH A SILVER LAYER

Judith Peñas Farré

Master's Degree in Nanoscience, Materials and Processes (2023-2024)

Supervisors: Dr. Nicolás Pazos Pérez, Dr. Luca Guerrini and, Prof. Xavier Mateos Ferré

Department of chemistry-physics and inorganic chemistry. Universitat Rovira i Virgili,

Campus Sescelades, Marcel·lí Domingo 1, Tarragona 43007, Spain

ABSTRACT: In recent years, gold and silver have been the most used plasmonic materials due to their optical properties, which vary depending on the composition, size and shape of the nanoparticles. This work presents the synthesis of star-shaped gold nanoparticles coated with a silver layer to obtain an improvement in the intensity of the signal they provide. The optical enhancing properties of gold nanostars coated with silver are characterized by UV-Vis, the shape with different quantity of silver are analyzed using transmission electron microscopy (TEM) and high resolution transmission electron microscopy (HRTEM), and to verify that the gold stars are coated with silver, elemental analysis is performed by means of energy dispersive X-ray (EDX) using a scanning transmission electron microscopy (STEM).

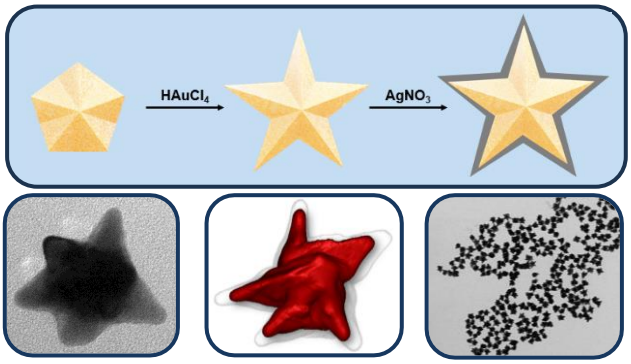

1. INTRODUCTION

The interaction of electromagnetic waves with nanoscale metals can induce collective oscillations of conduction electrons, known as localized surface plasmon resonances (LSPRs). [1] Such unique property of metallic nanostructured materials results in high local enhancements of the electromagnetic energy at their surfaces.[1] This opened new avenues for fundamental research and led to the development of an increasing number of applications in many fields (e.g., surface-enhanced spectroscopies, catalysis, plasmonic solar cells, nanodevices for bio-applications, photoacoustic imaging, etc.). Colloidal gold and silver nanoparticles are among the most common classes of plasmonic nanomaterials.

The plasmonic response of nanostructures is primarily influenced by their composition, size, and shape. Among these factors, the shape of individual nanoparticles, given a specific composition, is the most effective tool for tailoring and fine-tuning their optical resonance properties.[1–3] Notably, when the simple spherical geometry is modified to incorporate asymmetric features, new surface plasmon resonances emerge in the extinction spectrum, allowing tuning across a broader spectral range. Additionally, the presence of corners or tips on the nanoparticle surface creates localized areas of high electromagnetic enhancement, a phenomenon known as the "lightning rod effect."[1]

Among various nanostructures, gold nanostars (Au NSt) are currently considered some of the most efficient plasmonic nanomaterials for optical sensing applications, particularly in surface-enhanced spectroscopies such as surface-enhanced Raman spectroscopy (SERS). Indeed, Au NSt are colloidally stable nanoparticles capable of generating exceptionally strong electromagnetic fields at their sharp tips, making them highly effective as single-particle optical enhancers.[4]

Synthetic protocols for fabricating Au NSt can be broadly divided into two main categories: seedless and seed-mediated strategies, which commonly result

in one-step and two-step approaches. Seed-mediated methods, which involve using spherical seeds as nucleation points for the asymmetric deposition of additional Au° atoms, are typically preferred due to the enhanced control they offer over the shape and size of the nanostars.[4] In these methods, spikes form through the reduction of Au^{+} to Au^{0} at the twin boundaries of the spherical seeds, which possess well-defined multitwinned crystallographic structures. These twin boundaries are the most reactive regions and, as the spikes grow, new twin boundaries form, thereby leading to the development of more crystalline planes and, consequently, more spikes.[5]

Gold-based plasmonic nanoparticles are often favored over silver due to their superior chemical stability and the ease with which their plasmonic properties can be precisely tuned by adjusting their shape and size, something that is often difficult to achieve with silver. However, silver nanomaterials have the advantage of supporting strong LSPRs across a broader spectral range (~300–1200 nm), whereas gold is typically limited to the red-NIR region.[3] Thus, to enhance the plasmonic response of Au NSt, researchers have focused on selectively growing a silver layer on preformed gold nanostructures to generate bimetallic Au@Ag NSt.[6–10] Moreover, the formation of such a core-shell material can notably alter the optical properties and electronic structure of the silver layer due to the changes in the dielectric environment and the interaction of electrons across the interface.[11] Interestingly, a study by Feng et al[12] has demonstrated that when the silver shell thickness is maintained around 2-2.5 nm, electron enrichment in the silver layer significantly decreases its tendency to oxidize, thereby improving its chemical stability. Therefore, bimetallic Au@Ag nanostructures exhibit significant potential as plasmonic materials due to their enhanced chemical stability, flexibility for precise shape tuning, and stronger plasmonic response provided by the silver layer.[6,9,13]

Typically, the synthesis of Au@Ag nanostructures favors the deposition of silver at the central core of the gold nanostructure, leaving the tips minimally coated unless larger amounts of silver are added. However, this can significantly reshape the bimetallic composite, leading to a more spherical geometry with small spikes, which notably reduces the concentration of electromagnetic fields at the tips.[14]

In this work, we have carefully refined the synthetic protocol for the epitaxial growth of Ag on preformed Au NSt to achieve a relatively uniform external shell. This approach preserves the star shape while enabling the precise tuning the LSPRs over a 200 nm range.

2. EXPERIMENTAL SECTION

2.1. MATERIALS AND METHODS

Materials. Polyvinylpyrrolidone (PVP MW25000), gold (III) chloride trihydrate ($HAuCl_4 \cdot 3H_2O$, 99.9%), trisodium citrate dihydrate ($C_6H_5Na_3O_7 \cdot 2H_2O$, ≥99.5%,) absolute ethanol (EtOH, ≥99.9%,), dimethyl formamide (DMF, ≥99%), silver nitrate ($AgNO_3$, 99.9%), and ascorbic acid (AA, 99%), were obtained from Sigma-Aldrich. All reactants were used without further purification. Milli-Q water (18 $M\Omega cm^{-1}$) was used in all aqueous solutions, and all the glassware was cleaned with aqua regia before the experiments.

Synthesis of Spherical Gold Seeds. Spherical multitwined gold NPs seeds of approximately 15 nm in diameter were synthesized by the Turkevich method.[15] Briefly, the Au particles were prepared by boiling 150 mL of Milli-Q water using a condenser to prevent solvent evaporation. When it boils energetically, 3.3 mL of sodium citrate (0.1 M) were added. After 1 min, 250 µL of a 0.1 M $HAuCl_4$ aqueous solution was added under vigorous stirring. The solution was left to react for 1h with agitation and boiling. During this time, the color of the solution gradually changed from colorless to purple to finally become deep red.

Transfer to EtOH and Concentration of the Spherical Gold Seeds. After cooling, the Au seeds particles were transferred to EtOH using PVP as a phase transfer agent.[16] Concretely, the gold nanoparticles (150 mL) were added drop by drop into

a PVP ethanolic solution (35 mL, 5 mM) under vigorous stirring. The reaction mixture was left during 24h at room temperature to ensure that PVP adsorption on the gold nanoparticles surface was completed.

Finally, to transfer the PVP-stabilized particles into EtOH, the solution of the gold nanoparticles was evaporated to a total volume of 15 mL, the solution was then centrifuged (16000 rpm, 20 min) the supernatant was removed, and the Au nanoparticles were redispersed in ethanol to achieve a final Au concentration of 18.7×10^{-4} M.

Synthesis of Au Nanostars. Tips were grown on the gold seeds using a modification of the standard PVP/DMF approach.[17] To do this, 7 g of PVP were dissolved in 35 mL of DMF, after its complete dissolution, the mixtures were further sonicated for 30 min to assure homogeneity of the polymer in the solution. Next, an aqueous solution of $HAuCl_4$ (107 µL, 0.1 M) was added. Immediately after, 260 µL of the Au seeds in EtOH ($[Au^0] = 18.7 \times 10^{-4}$ M) were rapidly added, the solution was energetically shaken after each addition and left undisturbed overnight. Within 15 min a color change from pale red (from the spherical seeds) to deep blue (gold NSt) could be observed indicating the formation of Au NSt. The Au NSt were cleaned by 7 centrifugations steps, in the first one, the stars were diluted to the half with EtOH and were centrifuged for 40 min at 7500 rpm, the supernatant was removed, and the particles were resuspended in EtOH (40 mL). Then, in the 5 subsequent centrifugation steps, the solution was centrifuged for 10 min at 7000 rpm and redispersed in 40 mL EtOH. Finally, in the last centrifugation (10 min, 7000 rpm), the Au NSt were redispersed in 20 mL of EtOH. This solution was kept to further use them as NSt seeds for the growth of Ag on their surface. The Au NSt obtained had a final Au^0 concentration of 1.32×10^{-4} M and exhibited a maximum absorbance peak around 800 nm.

Coating the Au nanostars with a silver layer. The growth of the silver layer on top of the surface of the Au NSt was performed as follows. Silver nitrate ($AgNO_3$, 8 µL 0.01 M), were added to 2 mL of a mixture of EtOH / Milli-Q water at ratio of 3 (0.5 mL H_2O, 1.5 mL EtOH) containing sodium citrate (6 µL, 0.1 M), Au NSt seeds (426 µL, 1.32×10^{-4} M), and ascorbic acid (4.8 µL, 0.01 M). The solution was energetically mixed and left undisturbed overnight.

Influence of silver nitrate / ascorbic acid ratio. First, the influence of ascorbic acid concentration was tested by selecting a fixed concentration of $AgNO_3$ (1 µL, 0.01 M) and varying the added ascorbic acid (0.01 M) from 1 µL, 1.5 µL, 2 µL, 2.5 µL, 3 µL, 3.5 µL to 4 µL. All other parameters were kept constant. 0.5 mL H_2O, 6 µL sodium citrate (0.1 M), and 1 mL Au NSt (1.32×10^{-4} M). Once the reducing agent was optimized to avoid external nucleation the silver nitrate / ascorbic acid ratio was systematically changed as follows. A set of experiments were performed where the silver nitrate / ascorbic acid ratio was varied from 2.5, 2, 1.67, 1.43, 1.25, 1.1 to 1, meanwhile all other parameters were kept constant. 1.5 mL EtOH, 0.5 mL H_2O, 6 µL sodium citrate (0.1 M) and 426 µL Au NSt (1.32×10^{-4} M).

Effect of the H_2O / EtOH ratio. Since water is necessary to dissolve the $AgNO_3$, ascorbic acid and citrate, different ratios of H_2O / EtOH were tested to find the optimal proportions. To do that, all parameters were kept constant 1 µL $AgNO_3$ (0.01 M), 6 µL sodium citrate (0.1 M), 214 µL Au NSt (1.32×10^{-4} M), and 4 µL ascorbic acid (0.01 M). Meanwhile the H_2O / EtOH ratio was varies from 0.7, 0.81, 1.5, 1.85, 2.3, 3 to 9.

Influence of sodium citrate. The influence of sodium citrate concentration on the silver growth was performed by maintain all parameters already optimized and changing the added amount of a sodium citrate (0.1 M) solution from 4 µL, 5 µL, 6 µL, 7 µL to 8 µL.

Influence of Au stars concentration used as seeds. The influence of the Au stars concentration used as seeds tested by maintain all parameters already optimized and changing the concentration of Au Nanostars added in EtOH from 5.16 x 10^{-5} M, 5.68 x 10^{-5} M, 6.20 x 10^{-5} M, 6.72 x 10^{-5} M, 7.75 x 10^{-4} M, to 9.30 x 10^{-4} M. If the total volume of the solution (2 mL) is considered, the concentrations of Au NSt added are as follows: 3.87 x 10^{-5} M, 4.26 x 10^{-5} M, 4.65 x 10^{-5} M, 5.03 x 10^{-5} M, 5.81 x 10^{-5} M, 6.97 x 10^{-5} M.

Influence of PVP concentration. The influence of PVP was tested by maintain all parameters already optimized and changing the concentration of PVP added from 0.1 mM, 0.15 mM, 0.2 mM, 0.25 mM, 0.3 mM, 0.35 mM to 0.4 mM. To assure minimal residual PVP on the Au NSt nine centrifugation steps were performed before performing the experiments.

Characterization. UV-Vis spectroscopy (Cary varian 5000), transmission electron microscopy (TEM, JEOL 1011 operating at 100 kV), high resolution transmission microscopy (HRTEM, JEOL F200 operating at 200 kV) and scanning transmission electron microscope (STEM, JEOL F200 operating at 200kV) were used to characterize the optical response, the size and the composition of the nanoparticles. TEM and HRTEM samples were prepared by drying a drop of the nanoparticle suspension directly on carbon−Formvar-coated 200 mesh copper grids or cooper carbon holey grids.

3. RESULTS AND DISCUSSIONS

To obtain the optimal conditions for the synthesis of Au NSt coated with a homogeneous silver layer different parameters were systematically varied during the synthesis.

Influence of silver nitrate. In previous studies[18] it has been shown that when silver is added on top of gold, it modifies the LSPRs to shorter wavelengths. This is because due to the different molar absorption coefficients of both materials.[19] For instance, spherical silver nanoparticles exhibit resonances around 400 nm, meanwhile spherical gold is around 500 nm.[20] Therefore, if silver is grown on top of the gold, depending on the amount added the plasmon will shift. This fact has been proved, by preparing a series of 7 samples where different amounts of silver nitrate (0.1 M) were added, keeping the other parameters the same in all samples. As can be seen in Figure 1, as more silver is added, the plasmon resonance is progressively shifted towards the blue spectral region.

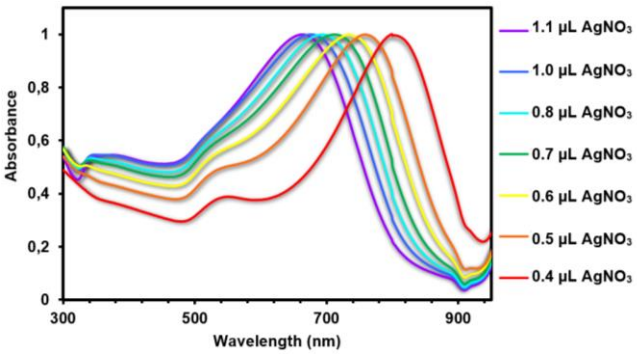

Figure 1. UV-Vis spectra showing the influence of silver nitrate.

Influence of ascorbic acid. The main function of ascorbic acid is to reduce silver ($Ag^+ \rightarrow Ag^0$). However, special care must be taken to avoid silver nucleation the bulk solution. To optimize this parameter a series of 10 samples were prepared where the amount of ascorbic acid (0.1 M) that was added was systematically varied. So, as more ascorbic acid was added, more silver was reduced and added to the surface of the stars. Therefore, the surface plasmon resonance was shifted more towards shorter wavelengths as more ascorbic acid was added meanwhile maintaining constant the $AgNO_3$ concentration (Figure 2). In addition to the plasmon displacement, another important factor to take into consideration, is to avoid external Ag nucleation. Therefore, the spectral region around 400 nm must be monitored since ion the plasmon of spherical Ag NPs is in this region. Therefore, as shown in Figure 2, the absence of it is an indicative that there is no Ag nucleation.

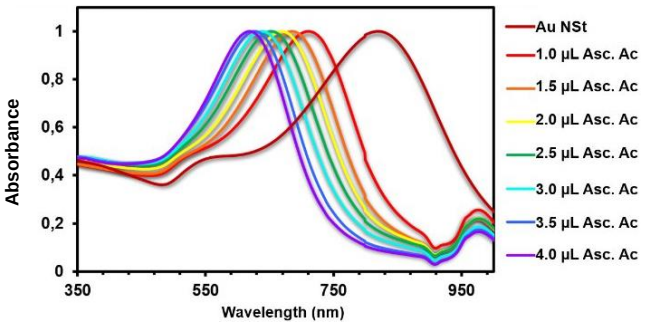

Figure 2. UV-Vis spectra showing the influence of ascorbic acid.

Influence of the H_2O / EtOH ratio. After the synthesis the Au NSt are stable in EtOH, however, the $AgNO_3$, the ascorbic acid, and the sodium citrate are soluble in water but not in EtOH. Therefore, a mixture of both solvents is required for the Ag overgrowth. To know the optimal relation of water and EtOH that must be added, a set of synthesis was made using different H_2O / EtOH ratios keeping the other parameters unchanged. UV-Vis spectrometry was used to characterize the samples. As shown in Figure 3, the optimal H_2O / EtOH ratio was 3, because the plasmon peak obtained is the one that maximizes its intensity.

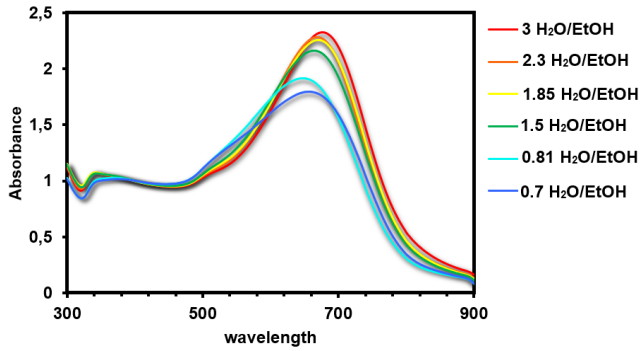

Figure 3. UV-Vis spectra influence of H_2O / EtOH ratio.

Influence of sodium citrate. Sodium citrate is a typical stabilizing agent for aqueous plasmonic colloids [21] that has been also used for the synthesis of aqueous Au NSt.[4,5,22] Therefore, since the developed synthetic protocol requires a part of water as solvent, sodium citrate has been incorporated. To find out if its addition is necessary, and the optimal quantity, five samples were synthesized with different amounts of sodium citrate. In Figure 4 it can be observed that when no citrate is added the shape of the UV-Vis spectra loses the typical morphology of the NSt, and as more sodium citrate is added, the shape of the spectra progressively retains the characteristic shape presenting only a blue shift in the plasmon resonance. However, this effect is only observed up to the addition of 6 µL, which is the optimal value, since at higher volumes of sodium citrate, a decrease in the intensity of the plasmon start to be observed. This effect is probably due to the stability provided by the sodium citrate. For lower amounts, the plasmon widens and has a lower intensity, indicating that the NSt morphology is changing. Thus, there is not enough citrate to stabilize the NSt. For higher amounts of citrate, a similar trend is observed which is probably due to an increase in the ionic strength of the media promoting again a system destabilization.

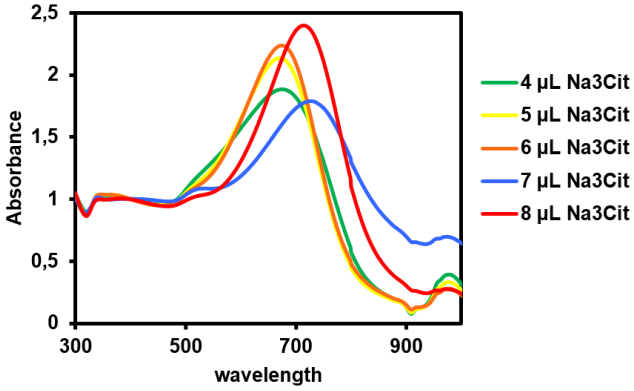

Figure 4. UV-Vis spectra influence of sodium citrate.

Influence of star concentration on silver growth. The amount of Ag that is reduced on top of the Au NSt is monitored by the blue shift of the plasmon resonance, generally this is controlled by the amount of Ag precursor added, however it can be also controlled by varying the number of seed particles added. To find out if the influence on the number of stars added is the same as the influence of $AgNO_3$, 7 samples were prepared, with different number of Au NSt. The results that could be observed were that the smaller number of stars were added, the plasmon came out more shifted towards the ultraviolet. On the other hand, the more stars were added, the plasmon came out shifted towards the infrared. These displacements are due to the fact that since the same

amount of silver was added for all the samples, if less amount of NSt were added then these ended up having much more silver around, since there was less amount of nanoparticles for the same volume of silver, on the other hand, if more stars were added, the silver was distributed more among the different stars and therefore, these ended up having a lower silver coating, it is for this reason that the plasmon resonance came out shifted to lengths of longer wavelengths. Confirming therefore the same trend as for the Ag precursor.

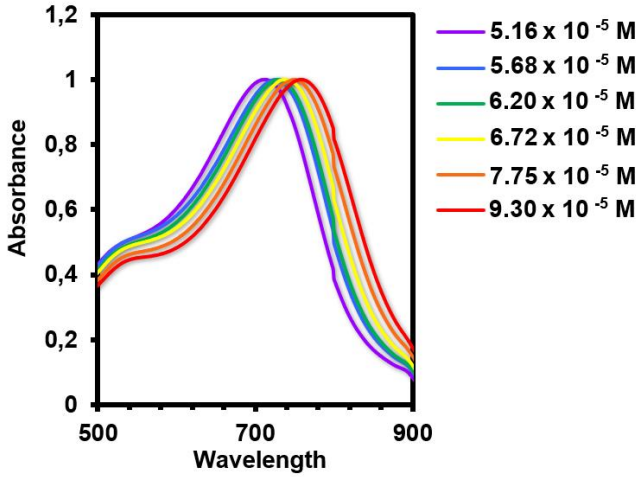

Figure 5. UV-Vis spectra influence of star concentration.

Influence of PVP on silver growth. The PVP acts as a stabilizer in the synthesis of gold NSt, and before the silver can be grown on the Au NSt, a cleaning process must be made in order to remove most of the PVP from the Au surface to allow that the Ag atoms can be deposited on it. However as has been shown already for the case of overgrowing Au NSt with Au, the amount of residual PVP is a key point in reduction and stabilization.[4] Therefore, to check if the PVP significantly affects the Ag overgrowth, an experiment was done using Au NSt that have been cleaned whit five centrifugation cycles and different amounts of PVP were added to each sample to evaluate the variation of the intensity. According to the UV-vis results (Figure 6) it was observed that the sample with lower amount of PVP was the one that shows the plasmon with higher intensity.

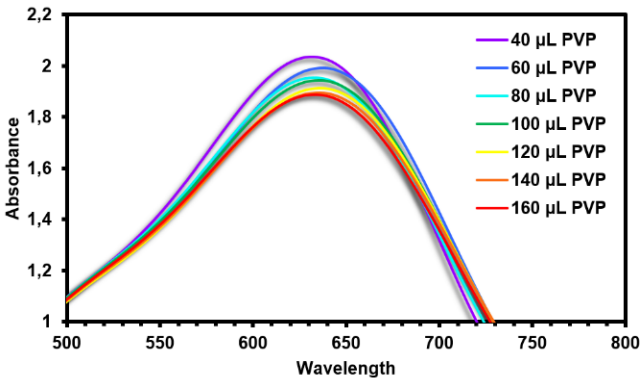

Figure 6. UV-Vis spectra influence of PVP.

Therefore, as it seems that less PVP shows the best results, an increase in the number of cleans of the Au NSt to remove the residual PVP remaining before growing the silver was performed. In this experiment stars were cleaned 5, 6, 7, 8, and 9 times prior to use them as seeds and were compared. According to figure 7 as more cleaning steps, more intense is the plasmon resonance of the NSt. This is because the residual PVP is reduced after each cleaning step. Despite these results, it is not possible to further clean the Au NSt without compromising their stability.

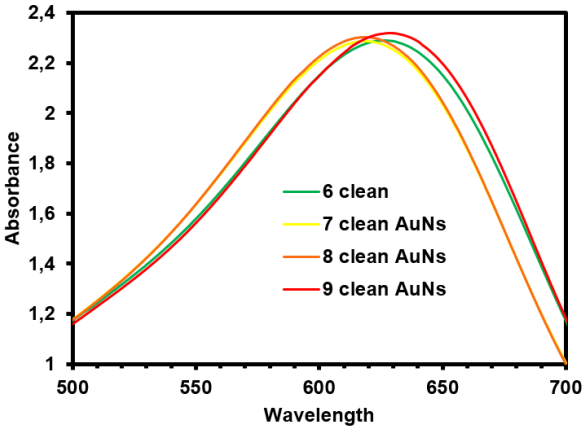

Figure 7. UV-Vis spectra Influence of AuNs cleans.

Optimized parameters for growing a silver layer on gold nanostars. Finally, by adjusting the above parameters, gold Nanostars with different silver layer thicknesses were obtained, where those with more silver were at shorter wavelengths, and those with more silver at longer wavelengths (see Figure 8). In the TEM images shown in Figure 8, it can be seen how as they change their optical response from infrared to

ultraviolet, as more silver is added, their spikes become rounded and wider.

To characterize these morphological changes The Ag coated Au NSt were systematically measured at different points. Figure 9 shows a schematic representation together with a graph showing the morphological variation of the gold NSt coated with a silver layer. Where it can be seen how the tip angle, the tip thickness, and the core diameter increase meanwhile the tip length decreases as more Ag is deposited on top of the Au NSt. In addition, the Ag thickness has been also measured at the cores, at the tips, and at the FWHM of the tips. In Figure 9 can be seen how these tree parameters increase as more Ag is added. However, meanwhile the thickness of the spikes at the sides and tips increase a maximum of around 4 nm, the core of the NSt increases almost the doble, around 8 nm.

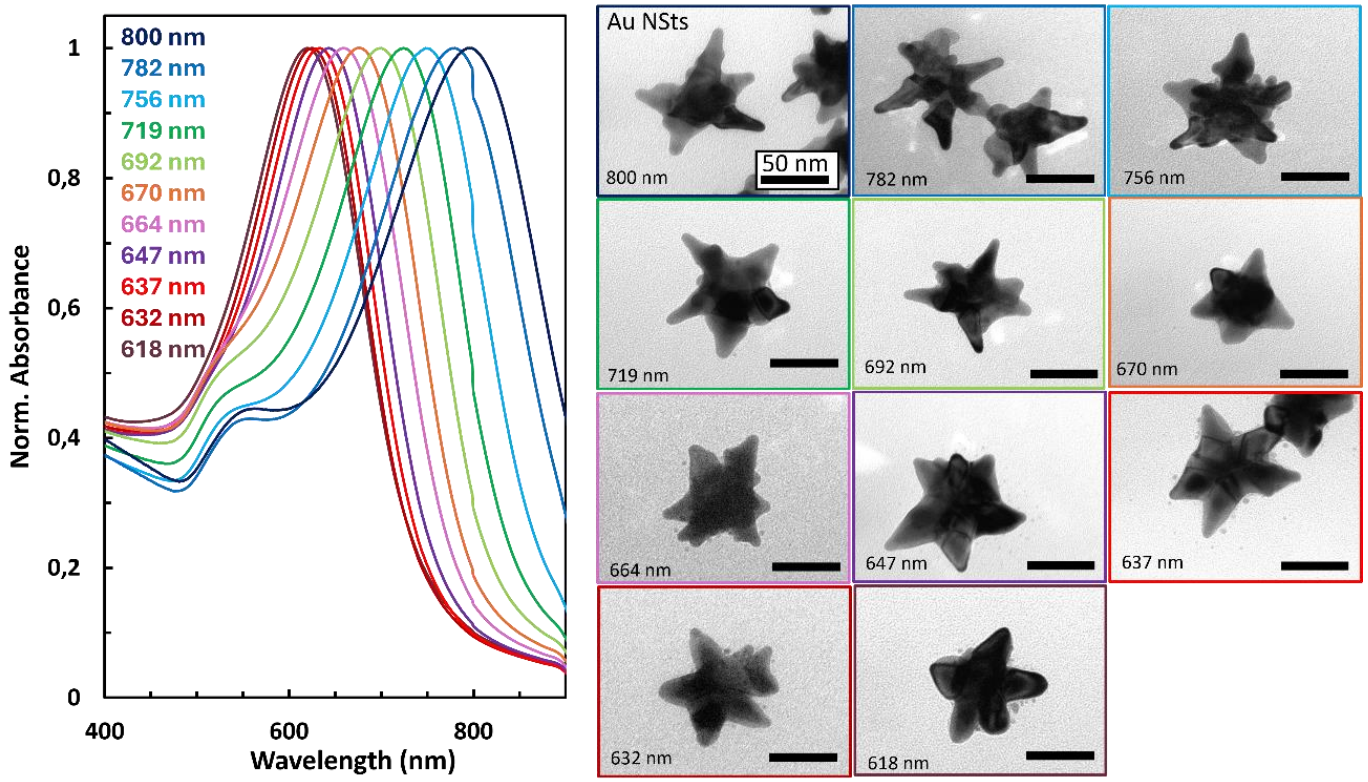

Figure 8. (A) UV-Vis spectra of different plasmons with different quantities of silver added. (B) Variation of nanostars depending on the amount of silver added.

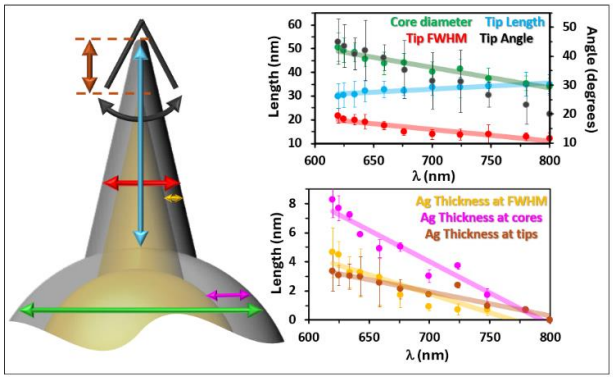

Figure 9. Schematic representation of morphology in silver variation.

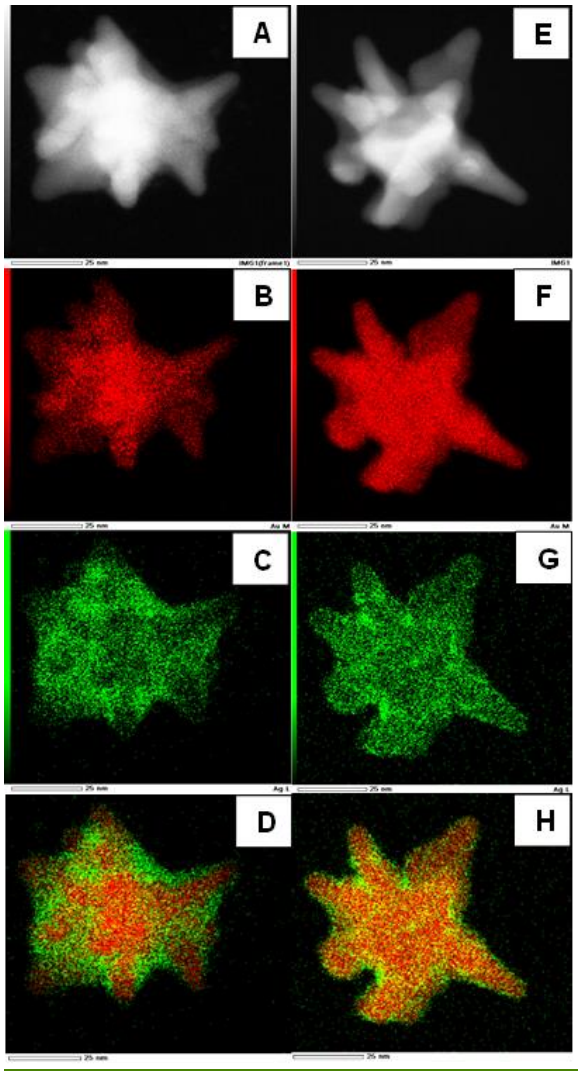

Figure 10. (A) Au-Ag Nanostar of 633 nm (B) Au composition of 633 nm Au-Ag Nanostar. (C) Ag composition of 633 nm Au-Ag Nanostar. (D) Representation of Au and Ag in the Au-Ag Nanostar of 633 nm. (E) Au-Ag Nanostar of 785nm. (F) Au composition of 785 nm Au-Ag Nanostar. (G) Ag composition of 785 nm Au-Ag Nanostar. (H) Representation of Au and Ag in the Au-Ag Nanostar of 785 nm.

Composition of gold Nanostars. To verify that the silver was around the gold NSt, and the morphological changes were not due to reshaping of the Au NSt, two selected samples, whit high and low amount of Ag with plasmon peaks located at 633 nm and 785 nm respectively, were characterized using scanning transmission electron microscopy (STEM). In figure 10 the different compositions of the two NSt can be seen, thus confirming that both samples had a silver coating and that the silver has maintained the morphology of the Nanostars. Through the EDX analysis, the ratio of elements in the NSt was quantified, revealing that the NSt with more Ag that has the plasmon at 632 nm has 40% silver and 60% gold, on the other hand, the NSt with less Ag with the plasmon resonance at 782 nm has a 10% silver and 90% gold.

4. CONCLUSIONS

In summary, we show the possibility of coating Au NSt with a thin layer of silver using a wet chemical approach through an epitaxial growth. This methodology allows a fine tuning of the optical response of spiked bimetallic NPs from the NIR to the visible range, while retaining a high plasmon efficiency. This plasmon tunability arises from a precise control of the deposition of silver in the sub 10 nm range during a seed-mediated process, where the seeds are standard Au NSt. Therefore, through the careful control of the reactant concentrations it is possible to finely control the thickness of the Ag layer and thus, the plasmon position meanwhile maintaining a spiky morphology. Optical, morphological and compositional characterization through UV-Vis, TEM and STEM indicates that the spikes became ticker, shorter, and rounded as more silver is grown, revealing that when their composition changes form 0%, to 10% to 45% of silver, their optical response changes respectively from 800 nm to 785 nm to 633 nm. Finally, the ability of having spiked colloidal structures whit a silver surface which in additionally it

is possible to fine control the plasmon position will provide new tools of applicability in many fields, such as biology, medicine, optics and plasmonic catalysis.

5. ACKNOWLEDGMENTS

I want to thank Nicolás Pazos for teaching, helping and guiding me throughout this work, Luca Guerrini for helping me with the measurements and Xavier Mateos for giving me the opportunity to do the TFM in his research group.

Project PID2022-141499OB-10, funded by MICIU/AEI/10.13039/501100011033/ and by FEDER/UE is acknowledged.

6. REFERENCES

(1) Giannini, V.; Fernandez-Dominguez, A. I.; Heck, S. C.; Maier, S. A. Plasmonic Nanoantennas: Fundamentals and Their Use in Controlling the Radiative Properties of Nanoemitters. *Chem Rev* **2011**, *111* (6), 3888–3912.

(2) Guerrini, L.; Graham, D. Molecularly-Mediated Assemblies of Plasmonic Nanoparticles for Surface-Enhanced Raman Spectroscopy Applications. *Chem Soc Rev* **2012**, *41* (21). https://doi.org/10.1039/c2cs35118h.

(3) Le Ru, E. C.; Etchegoin, P. G. *Principles of Surface-Enhanced Raman Spectroscopy*; Elsevier: Amsterdam, The Netherlands, 2009. https://doi.org/10.1016/B978-0-444-52779-0.X0001-3.

(4) Becerril-Castro, I. B.; Calderon, I.; Pazos-Perez, N.; Guerrini, L.; Schulz, F.; Feliu, N.; Chakraborty, I.; Giannini, V.; Parak, W. J.; Alvarez-Puebla, R. A. Gold Nanostars: Synthesis, Optical and SERS Analytical Properties. *Analysis & Sensing* **2022**, *n/a* (n/a), e202200005. https://doi.org/https://doi.org/10.1002/anse.202200005.

(5) Pazos-Perez, N.; Guerrini, L.; Alvarez-Puebla, R. A. Plasmon Tunability of Gold Nanostars at the Tip Apexes. *ACS Omega* **2018**, *3* (12). https://doi.org/10.1021/acsomega.8b02686.

(6) Atta, S.; Vo-Dinh, T. Bimetallic Gold Nanostars Having High Aspect Ratio Spikes for Sensitive Surface-Enhanced Raman Scattering Sensing. *ACS Appl Nano Mater* **2022**. https://doi.org/10.1021/ACSANM.2C02234.

(7) Lê, Q. T.; Ly, N. H.; Kim, M.-K.; Lim, S. H.; Son, S. J.; Zoh, K.-D.; Joo, S.-W. Nanostructured Raman Substrates for the Sensitive Detection of Submicrometer-Sized Plastic Pollutants in Water. *J Hazard Mater* **2021**, *402*, 123499. https://doi.org/10.1016/j.jhazmat.2020.123499 .

(8) Quang, A. T. N.; Nguyen, T. A.; Vu, S. Van; Lo, T. N. H.; Park, I.; Vo, K. Q. Facile Tuning of Tip Sharpness on Gold Nanostars by the Controlled Seed-Growth Method and Coating with a Silver Shell for Detection of Thiram Using Surface Enhanced Raman Spectroscopy (SERS). *RSC Adv* **2022**, *12* (35), 22815–22825. https://doi.org/10.1039/D2RA03396H.

(9) Benavides, L. N.; Moreno, M. S.; Murgida, D. H.; Castro, M. A. Porphyrin-conjugated Silver-coated Gold Nanostars for Ultrasensitive Detection and Multiplexing. *Journal of Raman Spectroscopy* **2020**, *51* (11), 2161–2170. https://doi.org/10.1002/jrs.5963.

(10) Parmigiani, M.; Schifano, V.; Taglietti, A.; Galinetto, P.; Albini, B. Increasing Gold Nanostars SERS Response with Silver Shells: A Surface-Based Seed-Growth Approach. *Nanotechnology* **2024**, *35* (19), 195603. https://doi.org/10.1088/1361-6528/ad25c9.

(11) Li, J. F.; Zhang, Y. J.; Ding, S. Y.; Panneerselvam, R.; Tian, Z. Q. Core-Shell

Nanoparticle-Enhanced Raman Spectroscopy. *Chem Rev* **2017**, *117* (7), 5002–5069. https://doi.org/10.1021/ACS.CHEMREV.6B00596/ASSET/IMAGES/LARGE/CR-2016-005967_0041.JPEG.

(12) Feng, Y.; Wang, G.; Chang, Y.; Cheng, Y.; Sun, B.; Wang, L.; Chen, C.; Zhang, H. Electron Compensation Effect Suppressed Silver Ion Release and Contributed Safety of Au@Ag Core-Shell Nanoparticles. *Nano Lett* **2019**, *19* (7), 4478–4489. https://doi.org/10.1021/ACS.NANOLETT.9B01293/ASSET/IMAGES/LARGE/NL-2019-012934_0006.JPEG.

(13) Zhu, J.; Chen, X. H.; Li, J. J.; Zhao, J. W. The Synthesis of Ag-Coated Tetrapod Gold Nanostars and the Improvement of Surface-Enhanced Raman Scattering. *Spectrochim Acta A Mol Biomol Spectrosc* **2019**, *211*, 154–165. https://doi.org/10.1016/J.SAA.2018.12.001.

(14) Joseph, D.; Baskaran, R.; Yang, S. G.; Huh, Y. S.; Han, Y. K. Multifunctional Spiky Branched Gold-Silver Nanostars with near-Infrared and Short-Wavelength Infrared Localized Surface Plasmon Resonances. *J Colloid Interface Sci* **2019**, *542*, 308–316. https://doi.org/10.1016/J.JCIS.2019.01.132.

(15) J. Am. Chem. Soc. 1963, 85, 3317−3328; Discuss. Faraday Soc. 1951, 11, 55−75

(16) Langmuir 2003, 19, 6693−6700

(17) Comm. Phys. 2018, 1, 13.; Nanotechnology 2008, 19, No. e015606; ChemPhysChem 2012, 13, 2561−2565; ACS Omega 2018, 3, 17173−17179).

(18) Feng, L.; Gao, G.; Huang, P.; Wang, K.; Wang, X.; Luo, T.; Zhang, C. Optical Properties and Catalytic Activity of Bimetallic Gold-Silver Nanoparticles. *Nano Biomedicine and Engineering*. Open Access House of Science and Technology 2010, pp 258–267. https://doi.org/10.5101/nbe.v2i4.p258-267.

(19) Dengler, S.; Kübel, C.; Schwenke, A.; Ritt, G.; Eberle, B. Near- and off-Resonant Optical Limiting Properties of Goldsilver Alloy Nanoparticles for Intense Nanosecond Laser Pulses. *Journal of Optics (United Kingdom)* **2012**, *14* (7). https://doi.org/10.1088/2040-8978/14/7/075203.

(20) Link, S.; Wang, Z. L.; El-Sayed, M. A. Alloy Formation of Gold-Silver Nanoparticles and the Dependence of the Plasmon Absorption on Their Composition. *Journal of Physical Chemistry B*. American Chemical Society May 6, 1999, pp 3529–3533. https://doi.org/10.1021/jp990387w.

(21) Dzhagan, V.; Kapush, O.; Plokhovska, S.; Buziashvili, A.; Pirko, Y.; Yeshchenko, O.; Yukhymchuk, V.; Yemets, A.; Zahn, D. R. T. Plasmonic Colloidal Au Nanoparticles in DMSO: A Facile Synthesis and Characterisation. *RSC Adv* **2022**, *12* (33), 21591–21599. https://doi.org/10.1039/d2ra03605c.

(22) Morla-Folch, J.; Guerrini, L.; Pazos-Perez, N.; Arenal, R.; Alvarez-Puebla, R. A. Synthesis and Optical Properties of Homogeneous Nanoshurikens. *ACS Photonics* **2014**, *1* (11), 1237–1244. https://doi.org/10.1021/ph500348h.